

Abnormal Pore Pressure Prediction Using Modified Eaton Model. A Case of Zeta Field, Onshore-Shelf, Niger Delta Basin

I. A. Okocha, L. I. Mamah, C. G. Okeugo

Department of Geology, University of Nigeria, Nsukka, Nigeria

Received November 20, 2019; Accepted March 21, 2020

Abstract

This study presents an alternative model for the prediction of possible over pressured reservoirs in a well yet to be drilled in Zeta Field, onshore/shelf region of Niger Delta basin. The modified Eaton prediction model (MEPM) basically accounts for both stress related (disequilibrium compaction) and secondary overpressure mechanisms. The application of MEPM was aimed at predicting pore pressure in the three wells and comparing it with the predicted pore pressure using Eaton Prediction model (EPM) and the measured pressure using Return Formation Tester (RFT) data. In this study, three wells from two fault blocks (A and B) were analyzed and plots of compressional velocity versus effective stress were used to determine causative overpressure mechanisms and to predict pore pressures. The result showed that the MEPM closely matched with the measured pressure for all the wells unlike the EPM. Disequilibrium compaction (under compaction) was identified as the main overpressure mechanism in wells A and C while secondary overpressure mechanism (unloading by fluid expansion) was identified as the potential cause of overpressure in Well B. Results of the pressure-depth plot showed that MEPM when compared with the results of EPM and measured pressure showed that the MEPM predicted overpressures to within 5% error margin especially at depths of overpressure. Therefore, this study has shown that pore pressure estimation using the modified Eaton prediction model are safer for predicting pore pressures from other well logs in the Niger Delta Basin.

Keywords: Abnormal pore pressure; Eaton prediction model; Under-compaction; Disequilibrium compaction; Secondary overpressure mechanisms; Modified Eaton's prediction model.

1. Introduction

According to [1], pore pressure prediction is the ability to create models using numerical formulas that mimic the subsurface pressure profile. Predicting subsurface pore pressure profile is important as it plays vital role during exploration planning and drilling campaigns. For over a decade now, pore pressure prediction has been of interest to both the researchers and industry stakeholders considering its adverse effects when wrongly predicted. It is believed that increase or decrease in subsurface pressures can lead to abnormal pressures (under pressure or over pressure) depending on the hydrostatic pressure of the formation. Abnormal pore pressure exists when pressure in the formation is either significantly lower (under pressure) than the hydrostatic pressure or exceeds (over pressure) the hydrostatic pressure in the formation. According to [2] stated that factors such as under compaction, fluid volume increase or expansion, fluid migration and buoyancy, stress and compartmentalized lithology in an aqueous environment are linked to the root causes of over pressure in formation. Before and during drilling, occurrences of these factors poses great danger if not accurately predicted as they are major causes of geologic hazards and drilling incidents like loss of rig, increase in drilling time, loss of drilling mud, kicks and well blowouts, weakening of faults and attendant consequences [3-5]. In order to accurately predict the subsurface pore pressure regime, basic pressure concepts such as hydrostatic pressure, overburden pressure, formation pore pressure, mechanism of overpressure generation and ways in which different overpressure generating mechanism affect rock properties must be considered [6-8]. In the Niger Delta Basin,

several authors have reported cases of overpressure and its effects on hydrocarbon production [9-11]. Achieving success in pore pressure prediction before drilling campaign begins should depend on choosing appropriate models based on fundamental assumptions that changes in normal pore pressure are due to either compaction porosity or fluid movement. Oftentimes, these fundamental assumptions are based on Eaton prediction model [12], though, the choice of these models vary based on areas and not the cause of abnormal pore pressure. In many over-pressured fields, the Eaton prediction model is widely used and is believed to accurately predicts overpressures caused by stress related mechanism (disequilibrium compaction or under-compaction) but overestimate or underestimate pore pressure when compared to measured values; it is also believed that the Eaton prediction model does not account for the changes in normal loading curve between primary and secondary over pressure mechanism [13-15]. In this article, we demonstrate steps involved towards better prediction of overpressure and accounting for secondary mechanism using modified Eaton's model.

2. Geological background of the study area

The Zeta Field is located in the Greater Ughelli and Central Swamp depo belt of the Niger Delta basin (Fig 1a and b).

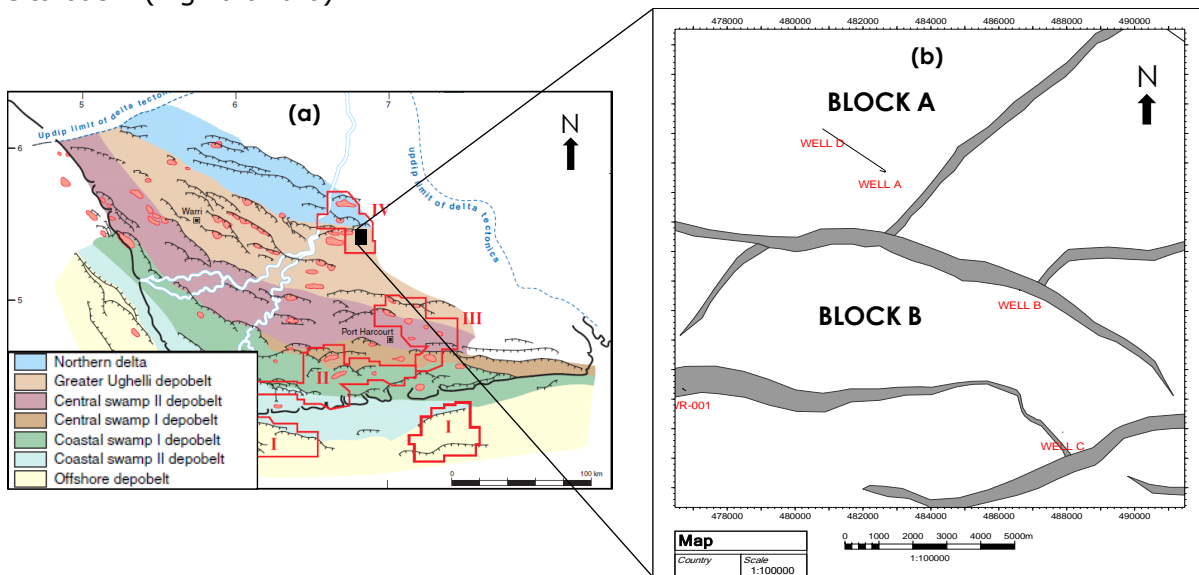


Fig 1a. A Niger Delta Basin view showing position of Zeta Field. (b) Map of Zeta Field showing well distributions and fault blocks (A and B)

This delta province contains only one identified petroleum system known as the Akata-Agbada petroleum system [16-17]. The target of oil exploration/exploitations within the basin is the Agbada Formation, which contains the best reservoirs. The three known lithostatigraphic units in the study area are from the bottom: the pro-delta facies of Akata Formation, paralic delta front facies of Agbada Formation and continental facies of Benin Formation (Fig. 1c). The Akata Formation is known as the oldest of the three formations with age ranging from Eocene to recent [18-19]. They occur as deep marine shale and serve as major source rock in the basin [20]. The Akata shales are typically under-compacted and overpressured with low density. The shales in some areas form diapiric structures including shale swells and ridges which often intrude into overlying Agbada Formation (Fig. 1d). It extends to the inland, exposing in north-eastern part of Niger Delta as the Imo shale. The Agbada Formation overlies the Akata Formation and constitutes the main reservoir and seal for hydrocarbons accumulation in the basin. The formation occurs throughout Niger Delta clastic wedge and has a maximum thickness of about 13,000 feet [21]. The lithologies consist of alternating sands, silts and shales, arranged within 10 –100 feet successions. They are defined by progressive upward changes in grain size and bed thickness.

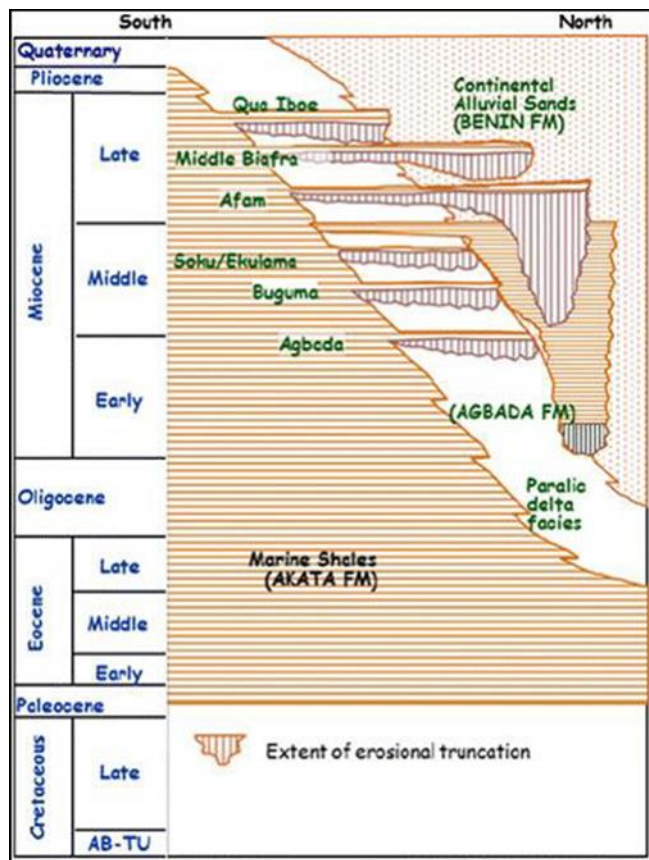


Fig 1c. Stratigraphy of the Niger Delta showing the lithologic units of the three formations. Modified from [19]

shown in Figs. 5. It has been reported [25] that well drilling in the field have had a series of setbacks with several drillable prospects abandoned due to possible blowout problems which as a consequence affected reserve estimation. This current study would help (i) highlight a better approach to predicting overpressure and (ii) understand the mechanical mechanism responsible for pressure regimes/distribution in the Zeta field.

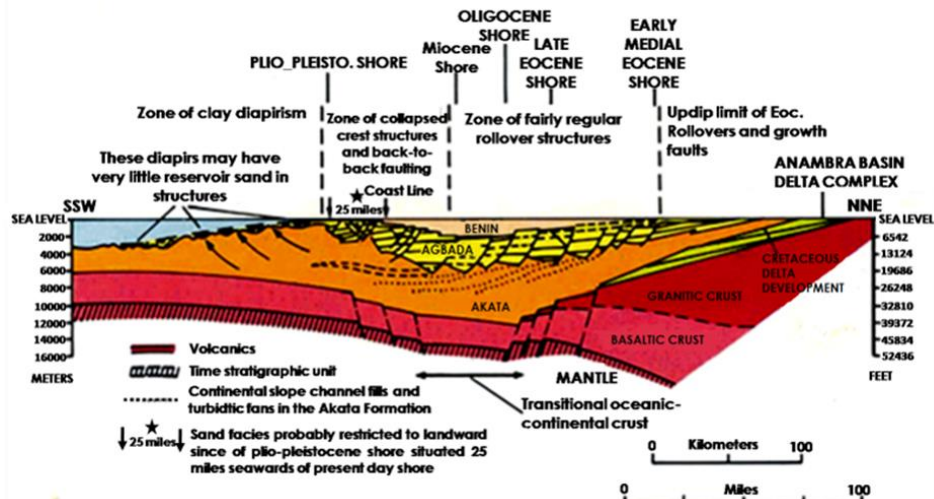


Fig 1d. Generalized dip section of the Niger Delta showing the structural provinces of the Delta. Modified from [30]

The strata are generally interpreted to have been formed in fluvial-deltaic environment. The top of the formation is recent, and the base is defined by the youngest marine shale. Although, shallow parts of the formation are composed entirely of non-marine sand deposited in alluvial or upper coastal plain environments during progradation of the delta [21]. The Benin Formation is the youngest and comprises the top part of the Niger Delta clastic wedge, from the Benin-Onitsha area in the north to beyond the coast line [20]. According to [22], the stratigraphic package of the study area is formed from a major regressive cycle that resulted in deposition of allocyclic units of transgressive marine sand, marine shale, shoreface and fluvial back swamp deposits. Structurally, the field is controlled by macrostructures such as simple rollover anticlines, multiple growth faults, antithetic and collapsed crest faults [22-24]. Locally, the deposited sequences encountered in the study area are characterized by proximal deltaic deposits and channel units that are separated by laterally extensive shale packages that represent flooding episodes, as

3. Pore pressure concepts and methods of prediction

Pore pressure concepts are based on the interaction between compaction process of sedimentary rocks and effective stress acting on the solid rock frameworks. Pore pressure have been attributed to different mechanism but the main ones are related to increase in effective stress and in-situ fluid generating mechanism [26], although the most commonly used pore pressure models in industry are based on the theory of normal sediment compaction described by [27]. Here the pore pressure models consider the behavior of porosity (or porosity indicators such as sonic interval transit time, resistivity or interval velocity) with depth to define the compaction disequilibrium a behavior known as Normal Compaction Trend (NCT). Sediment compaction processes affects porosity and greatly impacts on the velocity, resistivity, density profiles and rock properties [12]. It is believed that as a rock compacts, the porosity is reduced and the density increases, which also causes the bulk modulus and shear modulus to also increase because of increase in grain contact area and grain contact stress [26]. Using well log data, density, resistivity and sonic velocity data either continue to increase or remain constant after they depart from their normal trends. Figure 2 shows a pressure-depth plot illustrating the existence of other pore pressure mechanisms, which must be taken into account to improve pressure predictions.

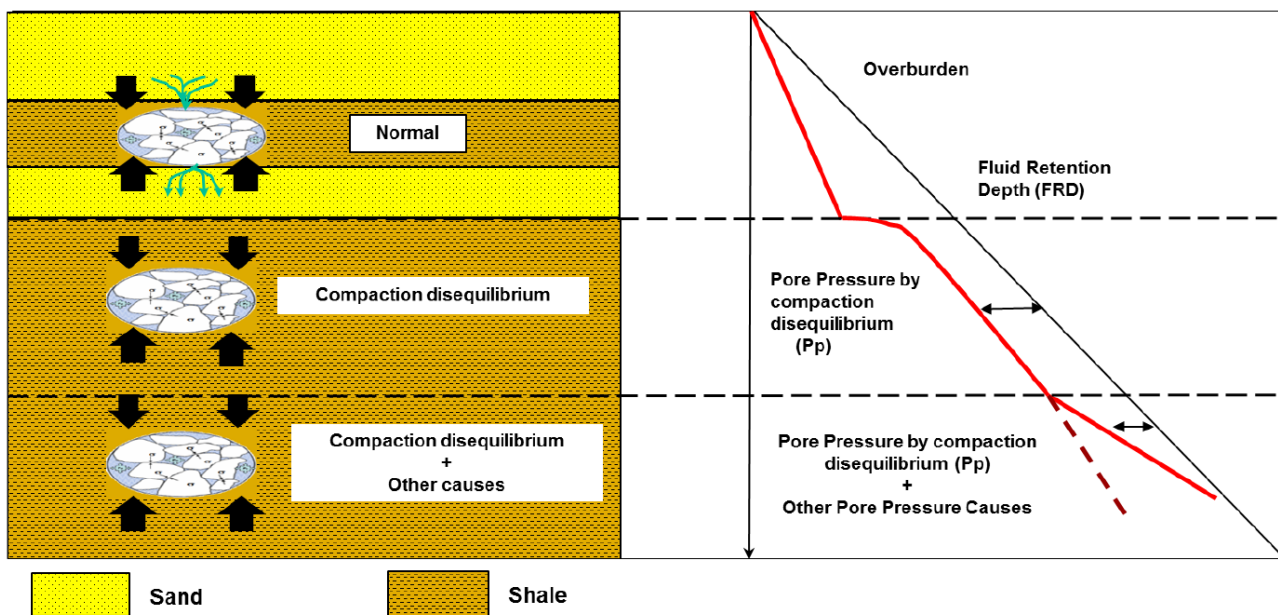


Figure 2. Pore pressure occur as combination of several mechanisms. Modified from [6]

According to [12], the causes of abnormal pore pressure are related to the loading and unloading process. It is believed that during the loading process, porosity decreases as the effective stress increases, so the interval transit time reduces and the formation density goes up. The relationship between the causes of over pressure, interval transit time, formation density and mechanical mechanism (loading and unloading process) are summarized in Table 1. In a case the formation has been compacted before the unloading process, the porosity cannot completely recover because the rock is elastic-plastic even as the effective stress decreases. Therefore, the interval transit time which is related to the rock conductive property would increase slowly and the formation density which is affected by the rock bulk property nearly remains unchanged with the assumption that the porosity and the acoustic velocity do not change if the rock is perfectly plastic as shown in Figure 3.

Table 1. Relationship between the causes of over pressure, mechanical mechanism interval transit time, formation density and prediction model. Modified after [12]

Cause of abnormal overpressure		Mechanical mechanism	Interval transit time	Formation density	Prediction model
The change of pore volume	Under compaction	Loading	Decrease	Decrease	Eaton Model
Structural tectonic movement	Compression from in-situ stress				Bowers loading model
	Shear from in-situ stress	Unloading	Decrease	Remain Unchanged	Modified Eaton Model
	Uplift of the formation				
The change of formation pore fluid volume	Aquathermal expansion	Unloading	Decrease	Remain Unchanged	Clay diagenesis
	Hydrocarbon Generation				Hydrocarbon Generation
	Fluids migration				Fluids migration
	Permeation				Permeation
	Hydraulic head				Hydraulic head

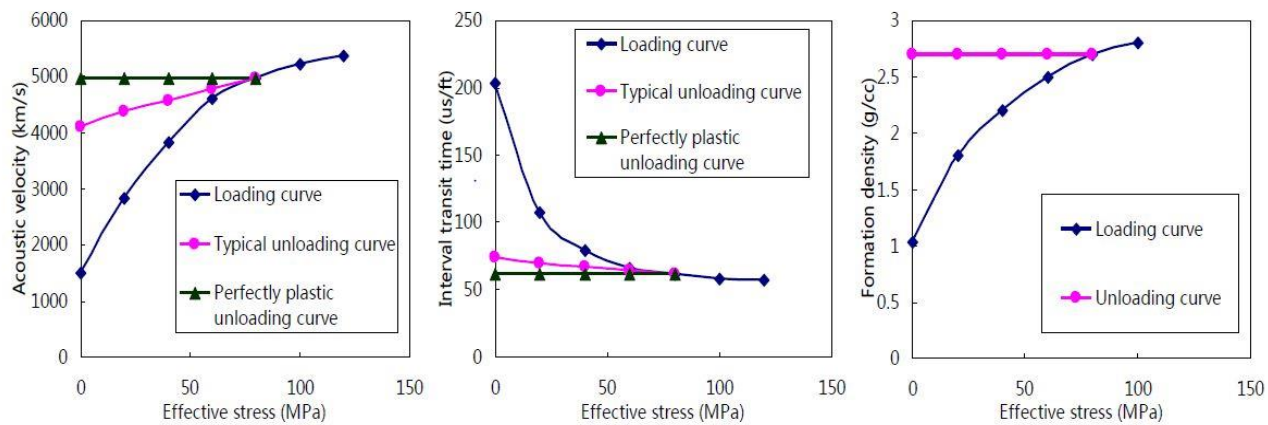


Figure 3. Response of logging data during loading and unloading. After [12]

3.1. The Eaton's pore pressure prediction model and it's modification

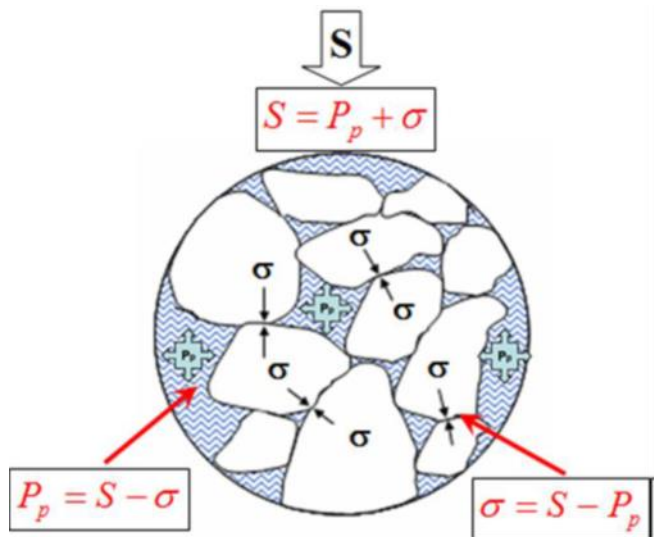


Fig. 4. Illustration of Terzaghi's Model of overburden stress distribution in rock-grains and fluid. Adopted from [15]

The methodology for generating any pore pressure prediction model is based on the relationship between porosity and effective stress or velocity and effective stress. Once effective stress (intergranular contact stress) and the vertical overburden stress is determined (Fig 4), pore pressure is calculated following the [28] model. The Terzaghi model states that if the vertical overburden stress, S increases with depth, Z and there is compaction disequilibrium at certain depth, the pore pressure, P_p must also increase starting in that depth as shown in Fig. (3). Therefore, pore pressure, P_p is defined as

$$P_p = S - \sigma \quad (1)$$

where: P_p = Pore fluid pressure; S = Vertical overburden stress; σ = Effective stress.

The overburden stress which is the combined weight of the rock matrix and fluids in the pore spaces overlying the formation at a specific depth; therefore it may be determined by means integral of bulk density of the sediments by:

$$S = g \int_0^z \rho_b(z) dz = \sum_i^n \rho_b g [Z_i - Z_{i-1}] \quad (2)$$

where: ρ_b = Depth dependent bulk density due to mechanical compaction; Z_i =Specific depth; Z_{i-1} = Specific depth before i ; g = Acceleration due to gravity.

It is known that the [29] prediction model for pore pressure prediction is an effective stress approach where effective stress σ is obtained from the Equation (3)

$$\sigma = \sigma_n \left(\frac{V_{ob(sh)}}{V_{n(sh)}} \right)^n \quad (3)$$

where: V_{ob} = Measured or observed shale velocity; V_n = Normal compacted shale velocity; σ_n = Normal effective stress; n = Eaton's exponent (describes the sensitivity of velocity to effective stress).

Substituting Equation (3) into (1), according to [28] equation and Eaton prediction model, pore pressure is estimated as:

$$P = S - (S - P_n) \times \left(\frac{V_{ob(sh)}}{V_{n(sh)}} \right)^3 \quad (4)$$

where: $\sigma_n = (S - P_n)$; P_n =Normal hydrostatic pressure.

Equation (4) is known as the Eaton's model equation which is popularly used to accounts for overpressure due to disequilibrium compaction.

In other to account for secondary mechanism such as fluid expansion and chemical compaction, a modified Eaton's model was thus generated to account for overpressure caused by unloading mechanisms. These mechanisms capture compaction process by tracing a different path from the normal compaction trend (NCT). In reality, effective stress controls compaction, and when used in Eaton's model is of no significance to secondary mechanisms of overpressure. To account for secondary overpressure mechanism using the modified Eaton's model, the effective stress is computed by determining a maximum effective stress from a virgin or loading curve (the highest reached before the occurrence of secondary mechanism) and substituting it for the normal effective stress in Eaton's model as follows:

$$\sigma = \sigma_{max} \left(\frac{V_{ob}}{V_n} \right)^{5.5} \quad (5)$$

Rather than Eq. 4, an effective stress for modified Eaton's model consists of two parts as shown:

$$\sigma = \sigma_n \left(\frac{V_{ob}}{V_n} \right)^{5.5} - \sigma_{max} \left(\frac{V_{ob}}{V_n} \right)^{5.5} \quad (6)$$

In this paper, Eq. 6 is used to predict pore pressure for both loading and unloading cases and the boundary conditions observed are:

(i) When undercompaction (loading) is the cause of overpressure, the second part of the equation vanishes because maximum effective stress has not yet been reached, so, the equation becomes

$$\sigma = \sigma_n \left(\frac{V_{ob}}{V_n} \right)^{5.5} \quad (7)$$

(ii) When secondary mechanisms are the cause of overpressure, the first part vanishes because compaction has ceased. This also shows that the rock has taken a trend different from the normal compaction trend. The equation then becomes

$$\sigma = \sigma_{max} \left[\frac{V_{ob}}{V_n} \right]^{5.5} \quad (8)$$

Pore pressure is then calculated by substituting either Eq. (7) and (8) into Eq. (1) depending on the overpressure mechanism as follows:

$$P = S - \sigma_n \left(\frac{V_{ob}}{V_n} \right)^{5.5} \quad \text{for under compaction} \quad (9)$$

$$P = S - \sigma_{max} \left[\frac{V_{ob}}{V_n} \right]^{5.5} \quad \text{for secondary mechanism} \quad (10)$$

3.2. Normal compaction trend (NCT)

The sonic velocity log were used to analyze the relationship between shale velocities and pressure, and to construct appropriate normal compaction trend. Shale velocity were generated along with vertical overburden stress. This was followed by generation of overburden stress and normal compaction trends from density log and sonic velocity log (Figs. 5). Formation hydrostatic pressure were calculated by multiplying the hydrostatic gradient (0.433 psi/ft) with the vertical depth. Velocity and vertical effective stress cross plot were used to determine the overpressure mechanisms in the selected wells. Pore pressure was calculated using equations (9) and (10) with prediction points picked from clean shale intervals because they are more responsive to overpressure than most clastic rock types. The predicted pressures were strictly compared with measured pressure from Repeat Formation Test (RFT) data and pressures predicted using Eaton's model.

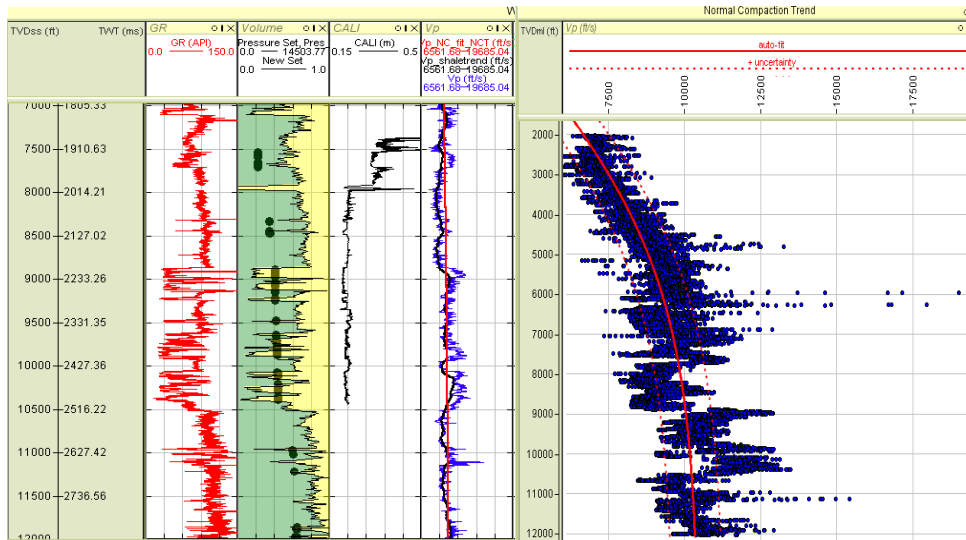


Figure 5a. Log suites with picked pressure points (black points in track 2) showing Normal Compaction Trend (NCT) in Well A

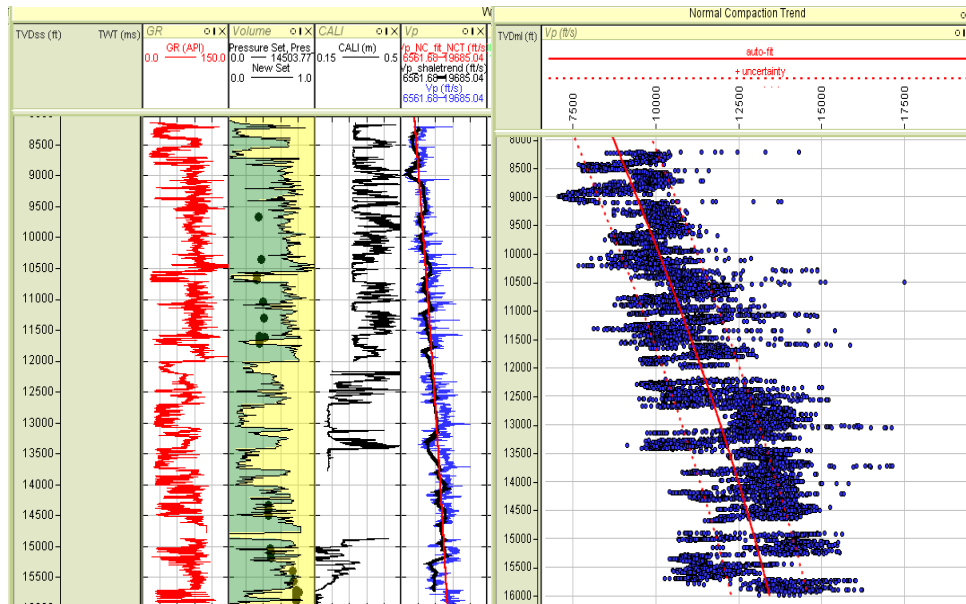


Figure 5b. Log suites with picked pressure points (black points in track 2) showing Normal Compaction Trend (NCT) in Well B

4. Results

The quantitative workflow stated above is implemented on real data set taken from three wells. In this section, pore pressure mechanisms, Eaton method and modified Eaton method of pore pressure prediction were utilized to characterize pressure conditions of wells in Zeta Field, onshore-shelf, Niger Delta Basin (Fig 1).

4.1. Determination of overpressure mechanism

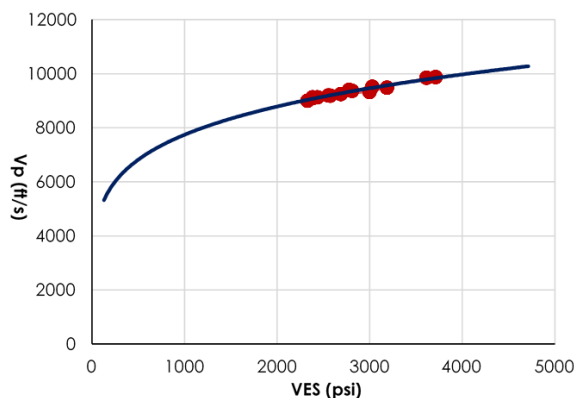


Fig. 6a. Velocity versus Effective stress cross plot for Well A

The results obtained from cross-plots of velocity and effective stress from three selected wells (A, B, and C) revealed that disequilibrium compaction or under-compaction is the source of overpressure in Wells A and C (Figs. 6a and 6c) with unloading (secondary mechanism) causing over pressure in Well B (Fig 6b). Observation showed that velocity, density and effective stress in wells A and C were lower than expected at normal pressure conditions at a given depth of burial. A sharp reversal was observed in Well B at depth of 15,200ft due to reduction in both velocity and effective stress which is an indication of secondary mechanism (unloading)

in the system. These results was confirmed following the fact that overpressure due to unloading cause rock or sediment properties to plot above and away from normal compaction curve while disequilibrium compaction scenarios plot on the normal compaction trend.

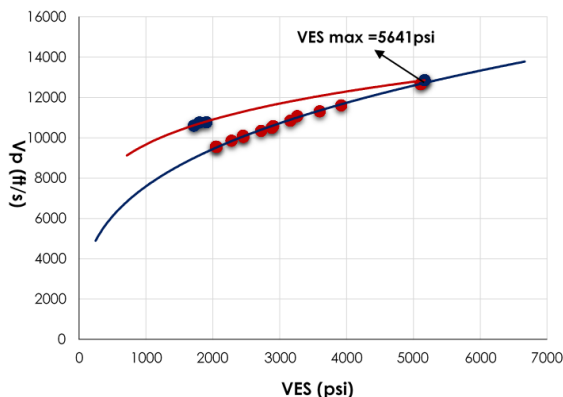


Fig. 6b. Velocity versus Effective stress cross plot for Well B

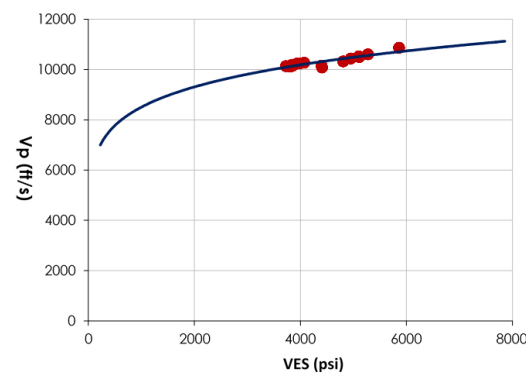


Fig. 6c. Velocity versus Effective stress cross plot for Well C

4.2. Pore pressure prediction

Pore pressures was predicted using the Eaton method and the modified Eaton's model. Equation (9) was employed for pore pressure prediction where disequilibrium compaction is the cause of overpressure while equation (10) was used where secondary mechanism is the cause of overpressure. The result of the analysis of pressure-depth plot for well A (Fig 7a) showed that the depth to top of overpressure started from 7800ft with pressure gradient ranging from 0.64 psi/ft to 0.7 psi/ft (mild to hard overpressure). The result of the modified Eaton predicted pressure and the measured pressure revealed good matching before the top of overpressure as shown in Fig. 7a. At depths less than 7,800ft (top of overpressure), pressure variations between the modified Eaton predicted pressure, Eaton predicted pressures and measured pressures were observed to have an average error difference of about 3%. At depths greater than 7,800ft, the Eaton predicted pressures showed closer consistency with

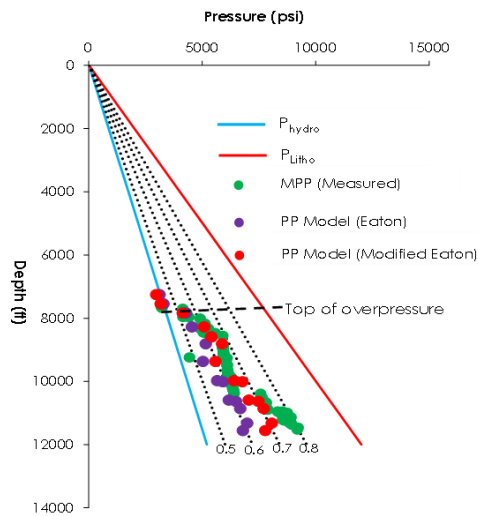


Fig. 7a. Pressure versus Depth Plot for Well A.
MPP= measured pressure, PPP = Predicted Pore
Pressure, P_{hydro} = Hydrostatic pressure, P_{litho} =
Lithostatic pressure

prediction pressure matched perfectly well with the measured pressures at all depth as shown in Fig 7b. Result confirmed close match of Eaton's prediction pressure with the predicted pressures of the modified Eaton from depth range of 9,000ft-15,000ft. At depths above 15,000ft, variations sets in with average error difference of about 9% between the modified Eaton and the Eaton predicted pressures. Similar trend was observed in Well C. The hydrostatic pressure gradient (0.43 - 0.46 psi/ft) was maintained to depth of 12,050ft which is the onset of overpressure as shown in Fig. 7c. After depth 12,050ft the measured pressure increased to the final depth with pressure gradient ranging between 0.65 and 0.68 psi/ft. During this time, the modified Eaton prediction pressure were matching consistently with the measured pressures while the Eaton prediction pressure showed non consistent trend with the modified Eaton prediction pressure and measured pressure with an average error difference of about 7% and 11%.

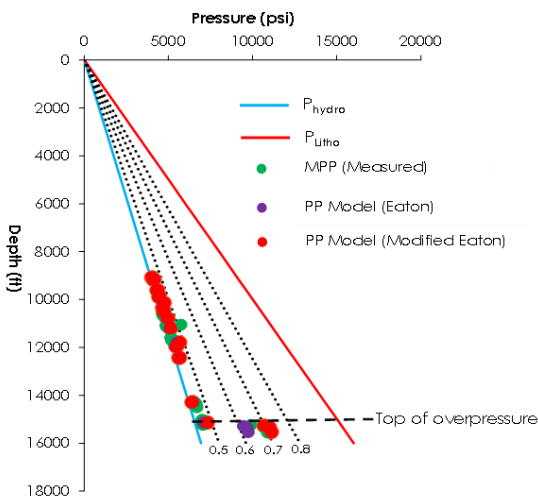


Fig. 7b. Pressure versus Depth Plot for Well B.
MPP= measured pressure, PPP = Predicted Pore
Pressure, P_{hydro} = Hydrostatic pressure, P_{litho} =
Lithostatic pressure

the modified Eaton predicted pressure but varies greatly at depths greater than 9,000ft especially when compared with the measured pressure. From Fig 7a, the average error difference between the Eaton predicted pressure with measured pressure and modified Eaton predicted pressure with measured pressure is about 14% and 9% respectively. This shows that consistent matching exists between modified Eaton prediction and measured pressure at depths greater than 9,000ft.

In Well B, pressure versus depth analyses showed that hydrostatic pressure was maintained with pressure gradient ranging from 0.433 psi/ft - 0.46 psi/ft between depths of 9000ft – 14,300ft. Top of mild overpressure (0.48psi/ft) was observed at depths between 14,500ft - 15,000ft (Fig 7b). This was followed by hard overpressure (0.7-0.72psi/ft) from the depth of 15,300ft to the stop depth. Observation showed that modified Eaton's

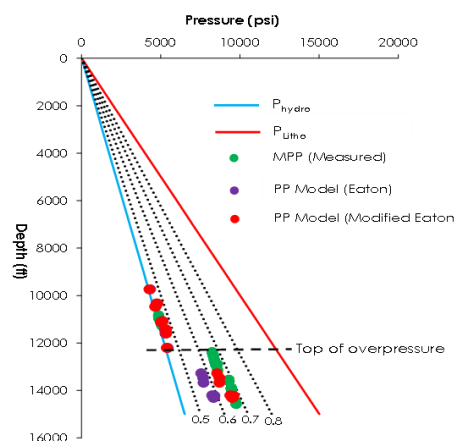


Fig. 7c. Pressure versus Depth Plot for Well C.
MPP= measured pressure, PPP = Predicted Pore
Pressure, P_{hydro} = Hydrostatic pressure, P_{litho} =
Lithostatic pressure

5. Conclusion

Understanding pressure behaviour before any drilling campaign is very crucial in any petroleum exploration business. Based on this study, pressure prediction was done using modified Eaton and Eaton prediction models. The results of the models were compared with the measured pressure model to understand which model has better matching consistency with the measured pressure data. Detailed analysis has confirmed that the onset of overpressure in wells A, B and C are 7,800ft, 14,500ft and 12,050ft respectively with over pressure ranging from mild to hard stage. Observation show that the mechanical mechanism responsible for over pressure in the field ranges from disequilibrium compaction (loading) to secondary mechanism (unloading). The result of cross plots between velocity and effective stress show disequilibrium compaction as the major source of overpressure in wells A and C, while secondary mechanism of overpressure was responsible for overpressure in well B. The results of the Eaton prediction model showed matching consistency with the results of the modified Eaton prediction model at depths of mild overpressure, while at deeper depths they vary greatly. It was observed that the modified Eaton prediction model for unloading (secondary mechanism) case, gave a better prediction than the Eaton's prediction model (disequilibrium compaction). This was confirmed by the result of error differences between the modified Eaton prediction model and measured pressure data and Eaton prediction model and measured pressure data. However, pore pressure estimation using the modified Eaton prediction model are safer for predicting pore pressure from other well logs in the Niger Delta Basin for optimum production and safer drilling campaign.

Acknowledgement

The authors wish to thank Shell Petroleum Development Company (SPDC), Port Harcourt; Petroleum Technology Development Fund (PTDF) Chair professor of Petroleum Geology, University of Nigeria, Nsukka (UNN), Prof. K.M Onuoha and Ikon Science for provision of datasets and enabling condition to publish this work.

References

- [1] Shaker SS. A New Approach to Pore Pressure Predictions: Generation, Expulsion and Retention Trio: Case Histories from the Gulf of Mexico. *CSEG Recorder*, 2015; 37: 44-51.
- [2] Swarbrick RE, Huffman AR, Bowers GL. Pressure regimes in sedimentary basins and their prediction. *Lead Edge*, 1999; 18: 511-513.
- [3] Holand P, and Skalle P. Deepwater kicks and BOP performance. SINTEF Report for U.S Minerals Management (2001).
- [4] Tobin HJ, Saffe, DM. Elevated fluid pressure and extreme mechanical weakness of a plate boundary thrust, Nankai trough subduction zone. *Geology*, 2009; 37(8): 679-682.
- [5] Zhang J. Effective stress, porosity, velocity and abnormal pore pressure prediction accounting for compaction disequilibrium and unloading. *Mar and Petrol Geol.*, 2013; 45: 2-11.
- [6] Bowers GL. Detecting high overpressure: The Leading Edge, 2002; 21: 174-177.
- [7] Swarbrick RE, Osborne MJ, Yardley GS. Comparison of overpressure magnitude resulting from the main generating mechanisms. In Huffman AR and Bowers GL., eds., *Pressure regimes in sedimentary basins and their prediction*. AAPG Memoir, 2002; 76: 1-12.
- [8] Tingay MRP, Hillis RR, Swarbrick RE, Morley CK, Damit AR. Origin of overpressure and pore pressure prediction in the Baram Province, Brunei. *AAPG Bull.*, 2009; 93(1): 51-54.
- [9] Nwozor KR, Omudu MI, Ozumba BM, Egbuachor CJ, Onwuemesi AG, Anike OI. Quantitative evidence of secondary mechanisms of overpressure generation: Insights from parts of Onshore Niger Delta, Nigeria. *J. Petrol. Technol. Dev.*, 2013; 3(1): 64-83.
- [10] Opara AI, Onuoha KM, Anowai C, Onu NN, Mbah RO. Geopressure and trap integrity predictions from 3-D data: Case study of the Greater Ughelli Depobelt, Niger Delta. *Oil Gas Sci Technol-Rev. IFP Energies Nouvelles*, 2013; 68(2): 383-396.
- [11] Ugwu GZ. Pore pressure prediction using seismic data: Insight from Onshore Niger Delta. *J. Geol. Min. Res.*, 2015; 7(8): 74-80.
- [12] Zijian C, Jingren D, Baohua Y, Qiang T, and Zhuo C. The Improvement Methods of Pore Pressure Prediction Accuracy in Central Canyon in Qiongdongnan Basin. *4th International Conf. on Environ. Energy and Biotech*, 2015; 85, doi:10.7763/IPCBEE.2015.

- [13] Zhang J. Pore pressure prediction from well logs: Methods, modifications, and new approaches. *Earth Science Reviews*, 2011; (1): 50-63.
- [14] Velázquez-Cruz D, Lopez-Solis VM, Díaz-Viera MA. Avances en la Determinación de Presiones Anormales en la Costa Mexicana del Golfo. *Revista Ingeniería Petrolera*, Diciembre del 2008, Vol. XLVIII, No.12.
- [15] Velázquez-Cruz D, Espinosa-Castañeda G, Díaz-Viera MA, Leyte-Guerrero F. New Methodology for Pore Pressure Prediction Using Well Logs and Divergent Area. *SPE Latin America & Caribbean, Petrol. Engi.* 2017, Conf., SPE-185557-MS, pp. 1-14.
- [16] Kulke H. Nigeria in Kulke, H. (Ed.) *Regional petroleum geology of the World, Part II: African, America, Australia and Antarctica*. Berlin, Gebruder Borntraeger, pp. 143-172 (1995).
- [17] Ekwezor CM, Daukoru EM. Northern delta depobelt portion of the Akata-Agbada petroleum system, Niger Delta, Nigeria. In: Magoon, L.B. and Dow, W.G. (Eds.) *The petroleum system from source to trap*. AAPG Memoir, 1994; 60: 599-614.
- [18] Reijers T, Petters S, Nwajide C. In: Selley RC (ed) *The Niger Delta Basin, African Basins—Sedimentary Basin of the World 3* Elsevier Science, Amsterdam, pp 151–172 (1997).
- [19] Lawrence SR, Monday S, Bray R. Regional geology and geophysics of the eastern Gulf of Guinea (Niger Delta to Rio Muni). *Lead Edge*, 2002; 21:1112–1117.
- [20] Short KC, Stauble AJ. Outline of geology of Niger Delta. *Am. Ass. Petrol. Geol Bull.*, 1967; 51:761–779.
- [21] Doust H, Omatsola E. Niger Delta. *Am. Ass. Pet. Geol. Bull.*, 1989; 48:201–238.
- [22] Reijers TJA. Stratigraphy and sedimentology of the Niger-Delta. *Geologos*, 2011; 17(3):133–162.
- [23] Evamy BD, Haremboure J, Kamerling P, Knaap W.A, Molloy FA, Rowlands PH. Hydrocarbon habitat of Tertiary Niger Delta. *Am. Ass. Pet. Geol Bull.*, 1978; 62:277–298.
- [24] Stacher P. Present understanding of the Niger Delta hydrocarbon habitat. In: Oti MN, Postma G (eds) *Geology of Deltas*. A.A. Balkema, Rotterdam, pp 257–267 (1995).
- [25] SPDC Internal Report: Onshore to deep water geologic integration, Niger Delta. In: Ejedawa J, Love F, Steele D, Ladipo K (eds) *Presentation packs of Shell Exploration and Production Limited*, Port-Harcourt (unpublished) (2007).
- [26] Chopra S, Huffman A. Velocity Determination for Pore Pressure Prediction. *CSEG RECORDER*, 2006: 28 – 46.
- [27] Terzaghi K and Peck RB. *Soil Mechanics in Engineering Practice*. John Wiley and Sons (1948).
- [28] Terzaghi K. *Theoretical soil mechanics in engineering practice*. Publ. by John Wiley and Sons, New York City, 556p (1943).
- [29] Eaton BA. The equation for geopressure prediction from well logs. *Soc. Petrol. Eng. of AIME* 1975, SPE 5544.
- [30] Whiteman A. *Nigeria: its petroleum geology, resources and potential*. Graham and Trotman, London, pp 394 (1982).

To whom correspondence should be addressed: Dr. C. G. Okeugo, Department of Geology, University of Nigeria, Nsukka, Nigeria, E-mail chukwudike.okeugo@unn.edu.ng